Atmos. Chem. Phys. Discuss., doi:10.5194/acp-2016-1143, 2017
Manuscript under review for journal Atmos. Chem. Phys.
Published: 2 January 2017


Atmospheric Chemistry and Physics Discussions

# Simultaneous measurements of new particle formation in 1-second time resolution at a street site and a rooftop site

Yujiao Zhu[1#], Caiqing Yan[2#], Renyi Zhang[2,3], Zifa Wang[4], Mei Zheng[2], Huiwang Gao[1], Yang Gao[1], Xiaohong Yao[1,5*]

[1]Key Lab of Marine Environmental Science and Ecology, Ministry of Education, Ocean University of China, Qingdao 266100, China

[2]State Key Joint Laboratory for Environmental Simulation and Pollution Control, College of Environmental Sciences and Engineering, Peking University, Beijing 100871, China

[3]Departments of Atmospheric Sciences and Chemistry, Center for the Atmospheric Chemistry and the Environment, Texas A&M University, College Station, TX 77843, USA

[4] State Key Laboratory of Atmospheric Boundary Layer Physics and Atmospheric Chemistry (LAPC), Institute of Atmospheric Physics, Chinese Academy of Sciences, Beijing, China

[5]Qiangdao Collaborative Center of Marine Science and Technology, Qingdao 266100, China

[#] both have the same contribution, * *Correspondence to*: Xiaohong Yao, Phone: (86) 532-66782565; Fax: 86-532-66782810; Email address: xhyao@ouc.edu.cn

Atmos. Chem. Phys. Discuss., doi:10.5194/acp-2016-1143, 2017
Manuscript under review for journal Atmos. Chem. Phys.
Published: 2 January 2017


Atmospheric Chemistry and Physics Discussions

**Abstract**

This study is the first time to use two identical Fast Mobility Particle Sizers for simultaneously measuring particle number size distributions (PNSD) at a street site and a rooftop site within 500 m distance in winter and spring times in Beijing. The obtained datasets in 1-second time resolution allow reasonably deducting the freshly emitted traffic particle signal from the measurements at the street site and thereby pave the way to study reduced or enhanced effects on new particle formation (NPF) in urban atmospheres through the site-by-site comparison. The number concentration of newly formed particles, i.e., smaller than 20 nm, and the NPF rate in the springtime were smaller at the street site than at the rooftop site. In contrast, NPF was enhanced in the wintertime at the street site with NPF rates increased by 3-5 times, characterized by a shorter NPF time and higher new particle yields than those at the rooftop site. Our results imply that the street canyon likely exerts distinct seasonal effects on NPF because of on-road vehicle emissions, i.e., stronger condensation sinks that may be responsible for reduced NPF in the springtime but efficient nucleation and partitioning of gaseous species that contribute to the enhanced NPF in the wintertime. We also analyzed the occurrence or absence of apparent growth for > 10 nm new particles. The oxidization of biogenic organics in the presence of strong photochemical reactions was argued to play an important role in growing >10 nm new particles, but sulfuric acid was unlikely the crucial specie for the apparent growth.

**Key words:** new particle formation, street site, enhanced nucleation, vehicle emissions, semi-volatile SOA

Atmos. Chem. Phys. Discuss., doi:10.5194/acp-2016-1143, 2017
Manuscript under review for journal Atmos. Chem. Phys.
Published: 2 January 2017


Atmospheric Chemistry and Physics Discussions

## 1. Introduction

New particle formation (NPF) has been measured under diverse environmental conditions, accounting for approximately 50% of the aerosol number production in the troposphere, but the chemical mechanism and species leading to aerosol nucleation and growth remain highly uncertain (Merikanto et al., 2009; Zhang et al., 2012). NPF occurs in two distinct stages, i.e., nucleation to form critical nuclei and subsequent growth of freshly nucleated particles to larger sizes (Kulmala et al., 2004, 2013; Zhang, 2010, 2012). In addition, the growth process competes with capture/removal of nanoparticles by coagulation with pre-existing aerosols. Currently, considerable uncertainty exists concerning the mechanism and the identity of chemical species responsible for aerosol nucleation and growth (Zhang et al., 2012; Wang et al., 2017). Sulfuric acid has been commonly considered as one of the main precursors of aerosol nucleation and growth, but is insufficient to explain the observed NPF under various ambient conditions (Kulmala et al., 2004, 2008; Zhang et al., 2012). Earlier studies indicated that $NH_3$ can enhance aerosol nucleation, but recent lab experimental and theoretical studies have suggested that amines and extremely low volatility secondary organics play vital roles in enhancing nucleation and promoting the initial growth of newly formed particles in the atmosphere (Zhang et al., 2004, 2009, 2012; Wang et al., 2010; Riipinen et al., 2011; Kulmala et al., 2013; Schobesberger et al., 2013; Ehn et al., 2014; Riccobono et al., 2014; Tröstl et al., 2016). Therefore, it is critical to evaluate the effects of nucleating species other than sulfuric acid and the dependence of NPF on pre-existing particles in the atmosphere. Urban street canyons provide semi-enclosed environments trapping vehicle exhausts that likely contain organics with different volatilities (e.g., oxalic, malonic, succinic, glutaric, adipic acid, and amines), $SO_2$, NOx, black carbon, etc. (Pierson et al., 1983; Stemmler et al., 2005; Burgard et al., 2006; Buccolieri et al., 2009; Ge et al., 2011; Sun et al., 2012), thus serving effectively as environmental chambers to investigation of the effects of on-road vehicle emissions, i.e., gaseous species and primary particles, on NPF.

A big challenge exits for studying NPF at street sites because of the interference from primarily emitted vehicular particles. The primary particles can be generated directly in the engine during fuel combustion or can be nucleated in the air during dilution and cooling of hot exhausts (Kittelson, 1998; Kittelson et al., 2008; Arnold et al., 2012; Rönkkö et al., 2013; Vu et al., 2015). The former primary particles consist mostly of soot and mainly exist in the Aitken mode and accumulation mode, ranging from 30 nm to 500 nm, and the freshly nucleated vehicular particles during the initial 1-2s exhaust cooling

Atmos. Chem. Phys. Discuss., doi:10.5194/acp-2016-1143, 2017
Manuscript under review for journal Atmos. Chem. Phys.
Published: 2 January 2017




and dilution processes reportedly exhibit a nucleation mode at 10-20 nm (Shi et al., 2000; Zhu et al., 2002a, b, 2006; Vu et al., 2015). The particle number concentration (PNC) at roadside can vary a lot, depending on the traffic flow, composition and speed as well as wind speed and direction (Yao et al., 2005). Scanning Mobility Particle Sizer (SMPS) and other scanning sizers, e.g, commonly operating in 5-10 minutes time resolution and occasionally down to 2-3 minutes, had been widely used to measure particle number size distributions (PNSD) at roadside. Dramatically varying PNC at roadside alone raise a challenge for accurately measuring PNSD using the low time-resolution scanning approach and the measured PNSD may severely distort from the real ones (Yao et al., 2006a, b). In addition, PNSD at roadside can also vary a lot because of the short distance between the sampling site and the traffic flow, e.g., the PNSD sometimes represent the overwhelming contribution from a single vehicle emission, but sometimes represent the combining contribution from a few vehicle emissions or the contribution from the traffic flow. Highly varying PNSD at roadside may further worsen the accuracy of the PNSD measured by low time resolution scanning sizers. When a high time resolution particle sizer, e.g., Fast Mobility Particle Sizer or Engine Exhaust Particle Sizer was used, the uncertainty can be greatly reduced (Yao et al., 2006a,b). The measured PNSD in 1-seond time resolution can allow extracting the new particle signal from the mixing signal of newly formed particles, pre-existing ambient particles and freshly emitted particles from combustion (Liu et al., 2014).

Ultrafine particles (<100 nm) have been reported to have adverse human health impacts through the destruction of the respiratory system (Oberdörster et al., 2004; Schlesinger et al., 2006; Zhang et al., 2015). On NPF days, the ultrafine particle number concentration is sharply increased and the health impact is largely dependent on the particle loading. Although a large quantity of studies focused on the effect of enhancement and scavenging on the occurrence and NPF rates, how enhancement and scavenging affects the net production of newly formed particles is still poorly understood. In addition, the newly formed particles inside a street canyon may become toxic when vehicles released organics is involved in the nucleation process.

In this study, we present simultaneous aerosol measurements at a street site and a rooftop site of 20-m high in winter and spring times in Beijing (Fig. 1). PNSD at these two locations were measured by two identical Fast Mobility Particle Sizers with 1-second time resolution. We focused on analyzing the differences in NPF rates and particle yields between the street

Atmos. Chem. Phys. Discuss., doi:10.5194/acp-2016-1143, 2017
Manuscript under review for journal Atmos. Chem. Phys.
Published: 2 January 2017


Atmospheric Chemistry and Physics Discussions

and rooftop sites, in order to evaluate the effects of street canyon on NPF. In addition, we also discussed the occurrence or absence of apparent growth in NPF events in terms of seasonal characteristics, potential condensation vapors, etc.

## 2. Method

### 2.1 Sampling sites, periods and meteorological conditions

Two urban sites, approximately 500 m away from each other, were adopted for sampling in this study (Fig. 1). One site was 18 m away from the curb of a heavy traffic (Chengfu) Road at the northwestern area in Beijing, which was physically located inside a street canyon. It was referred to as street site afterwards. The daily average traffic volume on this road was $1.9\times10^3$ vehicles $h^{-1}$ with the maximum of $2.2\text{-}2.4\times10^3$ vehicles $h^{-1}$ in morning and afternoon rush hours. A space-heating boiler with a stack in ~50 m height was approximately 200 m away from the street site at the northeast. The site on the rooftop of an academic building inside the campus of Peking University (~20 m above the ground level) was approximately 200 m away from the nearest Zhongguancun North Street. The site is referred to as the rooftop site in this study and was assumed to represent the urban background.

Two sampling campaigns were conducted in winter 2011 and spring 2012, respectively. The winter sampling in 2011 included two phases, i.e., 1) only one FMPS operated in 10-15 December at the street site; 2) two FMPS operated in 16-23 December at the street site and rooftop site, respectively. The weather is typically sunny and dry during the sampling campaign with surrounding air temperature from -9.5℃ to 12.8℃ (see Supplementary, Fig. S1).

In 12-17 April 2012, the two identical particle sizers were deployed at the rooftop site for inter-comparison. The simultaneous measurements at two sites started from 18 to 27 April 2012. The ambient temperature ranged from 8.2℃ to 31.5℃ during the spring sampling period (Fig. S1). Sunny days occurred on 12-17 April and 25-27 April 2012 with ambient RH below 55%. Either rainy or cloudy days occurred in the remaining 7 days.

### 2.2 Sampling Instruments

Two identical Fast Mobility Particle Sizers (FMPS, TSI Model 3091) downstream of two dryers (TSI, 3062) were used in this study. FMPS were used to continuously measure PNSD ranging from 5.6 nm to 560 nm in 1-second time resolution,

Atmos. Chem. Phys. Discuss., doi:10.5194/acp-2016-1143, 2017
Manuscript under review for journal Atmos. Chem. Phys.
Published: 2 January 2017




facilitating the investigation of rapid changes of nanoparticles due to formation and mixing from different sources (Yao et al., 2005, 2006b). Conductive tubes (TSI 3/8'') were used for the sampling lines, and the same total length (2.8 m) was kept for each site. The two FMPS operated side-by-side during 12-17 April 2012 for inter-comparison. The correlation coefficients ($R^2$) of the measured number concentrations between the two sizers were greater than 0.95 for particles between 9.3-107.5 nm, 0.81 for particles in the size bin of 8.06 nm. However, the correlation coefficients are fairly small (< 0.3) for the remaining two size bins (6.04 nm and 6.98 nm), thus are discarded in the analysis. The relative error between the two FMPS was less than 30% for 8.06-107.5 nm particles. Using a regression equation obtained in the inter-comparison, one FMPS was used as the reference to correct the number concentration measured by the other. The correction factors were listed in Table S1. Although the FMPS has the advantage of high time resolution, it has its own weakness. For instance, it was reported to underestimate the particle sizes compared to the SMPS and HR-ToF-AMS (Lee et al. 2013). In this study, the FMPS data were corrected based on a Condensation Particle Counter (CPC, TSI Model 3775) using the method developed by Zimmerman et al. (2015).

In addition to the two FMPS instruments measuring PNSD, a few other instruments were deployed at the same time. For example, $SO_2$, $NO_x$, NO, $O_3$, $CO_2$, CO were measured and recorded every minute at the rooftop site close to FMPS. Other available instruments, including aethalometer, DustTrak, Q-Trak photometer, CPC, were used for filter sampling or semi-continuously measuring air pollutants. A meteorological station was located on the roof of one sixth-floor building about 50 m from the street site, measuring air temperature, RH, wind speed and direction. The solar radiation was measured by State Key Laboratory of Atmospheric Boundary Layer Physics and Atmospheric Chemistry (LAPC) (Hu et al., 2010, 2012).

### 2.3 Computational Methods

In this study, particles less than 20 nm are defined as the nucleation mode (Kulmala et al., 2004). The apparent formation rate of new particles larger than 8 nm (NPF rate, $J_8$), taking consideration of the coagulation and growth losses, is calculated based on the Eq. (1) (Kulmala et al., 2012):

$$J_8 = \frac{dN_{8-20}}{dt} + CoagS_{8-20} \cdot N_{8-560} + \frac{GR_{8-20}}{12} \cdot N_{8-20} + S_{losses} \quad (1)$$

Atmos. Chem. Phys. Discuss., doi:10.5194/acp-2016-1143, 2017
Manuscript under review for journal Atmos. Chem. Phys.
Published: 2 January 2017


Atmospheric Chemistry and Physics Discussions

where the coagulation loss for particles with diameter of 8-20 nm ($CoagS_{8\text{-}20}$·$N_{8\text{-}560}$) is the sum of particle-particle inter- and hetero-coagulation rates calculated similarly to Yao et al. (2005). The growth loss is due to condensation growth ($GR_{8\text{-}20}$) out of the 8-20 nm size range during the calculation period. $S_{losses}$ includes additional losses and is assumed to be zero in this study.

The apparent growth rate (GR) of new particles is determined by the slope of the fitted geometric median diameter of new particles ($D_{pg}$, calculated as Whitby et al., 1978; Zhu et al., 2014) to the growth duration shown in Eq. (2):

$$GR = \frac{\Delta D_{pg}}{\Delta t} \quad (2)$$

The condensation sink is the loss rate of condensable vapor molecules onto the pre-existing particles, and calculated similarly to Dal Maso et al. (2005) and Kulmala et al. (2001, 2005):

$$CS = 2\pi D \int D_p \beta_M (D_p) n(D_p) dD_p = 2\pi D \sum_i \beta_M D_{pi} N_{pi} \quad (3)$$

where D is the diffusion coefficient, $\beta_M$ is the transitional regime correction factor, $D_{pi}$ is the particle diameter of size class i, and $N_{pi}$ is the particle number concentration in size class i.

Gas-phase sulfuric acid concentration is estimated based on global solar radiation (SR), $SO_2$ concentration and condensation sink (Petäjä et al., 2009):

$$[H_2SO_4] = k \cdot \frac{[SO_2] \cdot SR}{CS} \quad (4)$$

where $k$ is a constant value of $2.3 \times 10^{-9}$ $m^2 W^{-1} s^{-1}$. In this study, the mixing ratio of $SO_2$ was measured only on the rooftop as discussed in Section 2.2, and the $SO_2$ at the street site was assumed to be identical.

The contribution of sulfuric acid vapor to the particle growth from $D_{p0}$ to $D_{p1}$ can be expressed in Eq. (5) based on Kulmala et al. (2001):

$$R=([H_2SO_4]_{average}/C)\times 100\% \quad (5)$$

where $[H_2SO_4]_{average}$ is the mean concentration of $H_2SO_4$ during the entire growth period, and the concentration of condensable vapor (C) for particle growth from $D_{p0}$ to $D_{p1}$ is calculated following Kulmala et al. (2001).

Atmos. Chem. Phys. Discuss., doi:10.5194/acp-2016-1143, 2017
Manuscript under review for journal Atmos. Chem. Phys.
Published: 2 January 2017


Atmospheric Chemistry and Physics Discussions

## 3. Results and discussion

### 3.1 Overview of NPF events during two campaigns

The NPF events occurred frequently in the sampling days, 7 out of 16 days in spring 2012 and 7 out of 14 days in winter 2011 (Fig. 2), consistent with previous studies showing that spring and winter were the seasons with highest frequency of NPF events in Beijing (Wu et al., 2007; Wehner et al., 2008; Wang et al., 2017). At the rooftop site, during the spring campaign, the NPF rates in long-term NPF events (>1 hour) ranged from 1.9 to 12.2 particle $cm^{-3}$ $s^{-1}$ on average of 8.0±3.5 particle $cm^{-3}$ $s^{-1}$ (Table S2). Short-term NPF events (<1 hour) were observed only on 25 April with larger NPF rates of 14-49 particle $cm^{-3}$ $s^{-1}$. Two different growth patterns of new particles were observed, i.e., Class I was characterized by a typical "banana shape" growth and occurred on 12-14 and 16 April when the geometric median diameter of new particles ($D_{pg}$) increased from ~10 nm to 30-60 nm in 3-10 hours with the GR of 6.4±3.1 nm $h^{-1}$ (Fig. S2); Class II was observed on 15, 25 and 27 April and it was characterized by the initial $D_{pg}$ of new particles at ~11 nm and no apparent growth being observed during the next 6-8 hours until the signal of new particles dropped to negligible levels (Fig. 2a). These two growth patterns have been frequently observed in Beijing (Wehner et al., 2004, 2008; Shi et al., 2007; Wu et al., 2007). When the long-term NPF events were considered alone, there was no evident difference for the NPF rates between Class I and Class II. At the street site, NPF events were also observed on 25 and 27 April 2012 and the $D_{pg}$ maintained at ~11 nm for 6-8 hours without apparent growth, consistent with the observed phenomenon on the rooftop (Fig. 3 a,b,e,f). The NPF rates in long-term NPF events were 1.9 particle $cm^{-3}$ $s^{-1}$ at both sites on 25 April, and 10.2 particle $cm^{-3}$ $s^{-1}$ on the rooftop versus 8.1 particle $cm^{-3}$ $s^{-1}$ at the street site on 27 April (Table S2). Four short-term NPF events observed only on 25 April 2012 showed large differences (7%-50%) of NPF rates between the two sites.

On the 7 NPF days in winter, the NPF rates at the street site were 7.0±2.9 particle $cm^{-3}$ $s^{-1}$ (Table S2). The values were comparable to those in spring observed at the two sampling site. No apparent particle growth was observed through all these wintertime events when the $D_{pg}$ of new particles remained at ~11 nm (Fig. 2b). Simultaneous NPF events were observed at two sites on 21, 22 and 23 December 2011 and the NPF rates were 0.9, 1.9 and 0.8 particle $cm^{-3}$ $s^{-1}$ on the rooftop, which were only 1/6-1/4 of those corresponding values at the street site, i.e., 4.0, 7.9 and 4.4 particle $cm^{-3}$ $s^{-1}$ (Table S2).

Atmos. Chem. Phys. Discuss., doi:10.5194/acp-2016-1143, 2017
Manuscript under review for journal Atmos. Chem. Phys.
Published: 2 January 2017


Atmospheric Chemistry and Physics Discussions

### 3.2 Reduced NPF at the street site in the springtime

On 25 and 27 April 2012, long-term NPF events were simultaneously observed at the two sites and lasted for 6-8 hours (Fig. 3a,b,e,f). We first analyzed the stronger NPF on 27 April. The NPF event occurred around 09:37-09:40 (all of the times indicated in this paper are local standard time) and was strongly associated with the increased wind speed, i.e., from <1 m $s^{-1}$ at 08:00 to >6 m $s^{-1}$ after 09:45 (Fig. S3). The mixing ratio of $SO_2$ increased from 1.5 ppb to 3 ppb during the initial half hour of the event and then rapidly dropped down to <1 ppb for the remaining five hours (Fig. 3c). The wind almost constantly from the northwest during the entire event, which allowed roughly estimating that the NPF possibly occurred in cleaner atmospheres over the region scale of ~120 km (on basis of the product of the wind speed and the NPF event's duration). The nucleation mode PNC varied during the whole event with three peaks observed at ~10:20, ~11:30 and ~13:45, suggesting the heterogeneity of NPF in horizontal direction (Fig. 3c). NPF is usually determined by precursors including sulfuric acid vapor, amine and/or other low volatile species (Zhang et al., 2012; Kulmala et al., 2013; Ehn et al., 2014). The heterogeneity is expected because it was impossible for the precursors to be constant in the regional scale including urban, semi-urban and rural atmospheres. The NPF rate of 8.1 particle $cm^{-3}$ $s^{-1}$ at the street site was slightly lower than that of 10.2 particle $cm^{-3}$ $s^{-1}$ on the rooftop, further suggesting the heterogeneity of NPF in vertical direction. The condensation sinks were 1.2±0.37 ($\times 10^{-2}$ $s^{-1}$) and 0.75±0.21 ($\times 10^{-2}$ $s^{-1}$) for the street site and rooftop site, respectively (Table S2), with the higher condensation sink at the street site partially responsible for the lower NPF rate. There were obvious differences in the initial new particle burst time (defined as the time of nucleation mode particles reaching the maximum number concentration) between these two sites, i.e., 25 minutes at the street site and 36 minutes at the rooftop site, leading to a larger increase of nucleation mode PNC on the rooftop (Fig. 3c). This phenomenon was first observed in this study by adopting the high time resolution instruments, while it was impossible to detect this feature in the previous literature using low time resolution scanning approach. In order to estimate the net production of newly formed particles at the two sites, we define $t_{s0}$ ($t_{r0}$) as the time right before the apparent NPF at the street (rooftop) site and $t_{s1}$ ($t_{r1}$) as the time when the nucleation mode PNC reaches the maximum at the street (rooftop) site. The net maximum increase of nucleation mode PNC (NMIoNP) at the street site during the period of $t_{s1}$-$t_{s0}$ was reduced by 30% relative to that on the rooftop ($t_{r1}$-$t_{r0}$) (Fig. 3c,d), clearly indicating the reduced NPF at the street site.

Atmos. Chem. Phys. Discuss., doi:10.5194/acp-2016-1143, 2017
Manuscript under review for journal Atmos. Chem. Phys.
Published: 2 January 2017


Atmospheric Chemistry and Physics Discussions

On 25 April, NPF events were also associated with a high wind speed (Fig. S4). Due to the high time resolution of FMPS, four short-term NPF events together with one long-term NPF event were observed at both sites (Fig. 3e-h). Each short-term NPF event only lasted for a several minutes (e.g., 10:07-10:26, 10:27-10:36, 10:38-11:02, 11:40-11:50 in Fig. 3f) concurrently with spikes of $SO_2$ at 1-2 ppb, but the calculated NPF rates were high, i.e., 14-49 particle $cm^{-3}$ $s^{-1}$ at the rooftop site and 13-38 particle $cm^{-3}$ $s^{-1}$ at the street site. The short-term events strongly implied a key role of sulfuric acid vapor in NPF and the heterogeneity of NPF in both horizontal and vertical directions. The long-term NPF event lasted for ~8 hours with varying nucleation mode PNC, suggesting that the NPF likely occurred in cleaner atmospheres over the region scale of ~140 km in different NPF rates. It also showed a longer new particle burst time and higher PNC on the rooftop (Fig. 3g), similar to those observed on 27 April 2012. The NPF rates of 1.9 particle $cm^{-3}$ $s^{-1}$ were similar between the two sites. The calculated condensation sinks were 0.65±0.23($\times10^{-2}$ $s^{-1}$) and 0.16±0.02($\times10^{-2}$ $s^{-1}$) at the street site and rooftop site, respectively. The larger condensation sink at the street site was partially responsible for the reduced NPF during the three short-term events, but did not affect the NPF rate in the long-term NPF event. However, the NMIoNP at the street site was reduced by 24% mainly due to the shorter initial new particle burst time (Fig. 3h).

Fig. 4 shows the difference of PNC between the two sites in April, with the PNC at the street site subtracting the corresponding ones at the rooftop site. The difference was largely negative for particles <14 nm during the NPF periods on 25 and 27 April (color solid lines), also indicating the reduced NPF at the street site. In contrast, such a difference was slightly positive for particles <14 nm during the non-NPF days and during the morning rush hours on 25 and 27 April prior to the occurrence of NPF events (Fig. 4, dash lines), because of increasing contributions from on-road vehicles at the street site. The negative difference further indicated that NPF inside the street canyon was reduced, which could be due to more pre-existing atmospheric particles or higher NO concentrations as proposed by Wildt et al. (2014).

### 3.3 Enhanced NPF at the street site in winter

On 21-23 December 2011, NPF events were simultaneously observed at the rooftop site and street site with the NPF rates of 0.8-1.9 particle $cm^{-3}$ $s^{-1}$ and 4.0-7.9 particle $cm^{-3}$ $s^{-1}$, respectively (Figs. 5 and S5). The different NPF rates indicated

Atmos. Chem. Phys. Discuss., doi:10.5194/acp-2016-1143, 2017
Manuscript under review for journal Atmos. Chem. Phys.
Published: 2 January 2017


Atmospheric Chemistry and Physics Discussions

that NPF was greatly enhanced at the street site. However, larger condensation sinks were calculated at the street site ($1.3\times10^{-2}$ $s^{-1}$ at the street site and $0.45\text{-}0.98\times10^{-2}$ $s^{-1}$ at rooftop site, Table S2).

The strongest NPF event was observed on 22 December. The NPF event was initially observed at 09:40-09:45 at both sites (Fig. 5a-d) and was also apparently correlated with increasing wind speed (Fig. S6).The NPF was roughly estimated to occur in a semi-regional scale over ~50 km. The initial new particle burst time periods were different at two sites. For example, nucleation mode PNC at the rooftop site gradually increased from $0.2\times10^{4}$ particle $cm^{-3}$ at that time to the maximum value of $1.4\times10^{4}$ particle $cm^{-3}$ during the initial 2 hours (Fig. 5c). At the street site, vehicle emissions frequently influence the sampling site, leading to numerous spikes in PNC and large uncertainty in calculating the NPF rate. We thus used the 25% minimum coefficient of variation (CV) of PNC as an indicator to eliminate the vehicle spikes (see supplementary document for the calculation method). The approached results showed that the nucleation mode PNC rapidly increased with the initial 26 minutes and then decreased. The NPF rate of 7.9 particle $cm^{-3}$ $s^{-1}$ at the street site was three times larger than that of 1.9 particle $cm^{-3}$ $s^{-1}$ on the rooftop. The larger NPF rate at the street site was mainly associated with a shorter time for the new particle burst. The NMIoNP at the street site during the whole NPF event was about 50% higher than that on the rooftop (Fig. 5d). When the nulceation mode PNC at the street site reached the maximum, the corresponding PNC on the rooftop was only one-third of its own maximum value.

We also directly deducted the contribution of vehicle spikes using the second approach described in supplementary document. The newly obtained PNC at street site were shown in Fig. 6a. The results obtained from the new approach showed 1) the initial new particle burst time was 30 minutes, 2) the calculated NPF rate was 7.0 particle $cm^{-3}$ $s^{-1}$, and 3) the NMIoNP was 61% higher than that on the rooftop. The results reasonably agreed with the previous results using the 25% minimum CV (Fig. 6b). The two approaches strongly implied NPF being greatly enhanced at street site.

On 21 December 2011, the NPF event at the street site was also characterized by a shorter initial new particle burst time and a larger NPF rate (Fig. 5e-h). Using the 25% minimum CV approach, the NMIoNP at the street site was 24% higher than that on the rooftop (Fig. 5h). When the nucleation mode PNC at the street site reached the maximum, the corresponding PNC on the rooftop was only one-fifth of its own maximum value. The NMIoNP at the street site was 46% large than that at the

Atmos. Chem. Phys. Discuss., doi:10.5194/acp-2016-1143, 2017
Manuscript under review for journal Atmos. Chem. Phys.
Published: 2 January 2017




rooftop site on 23 December and didn't detail (Fig. S5). The second approach was invalid in the two days because of the weak NPF.

Again, we calculated the difference of PNC between the two sites in December 2011 using the number concentrations at the street site subtracting the corresponding concentration at the rooftop site (Fig. 7). On the strongest NPF day (22 December), the differences for <20 nm particles were positive during the NPF periods and approximately two hours prior to the NPF. The former difference was evidently larger than the latter. Recall, the difference was negative during the NPF periods in April 2012 (Fig. 4). The larger difference during the NPF period than prior to the NPF on 22 December was unlikely due to the low-ambient-temperature-favored stronger formation of primary vehicular particles during the initial 1-2 seconds dilution (Burgard et al., 2006; Bishop et al., 2010) and the poor dispersion condition because of the higher ambient temperature and larger wind speed during the NPF period. The differences for <20 nm particles during the NPF period on 22 December were also larger than the differences averaging over non-NPF days (17-19 December) in December and the average value observed on 20 December alone, when the most frequent spikes of vehicular particles occurred among all non-NPF days in December, at the corresponding particle size ranges. All these confirmed the NPF being enhanced at the street site on 22 December. When the vehicular particle spikes during the NPF on 22 December were eliminated using the 25% minimum CV approach, the newly obtained difference also confirmed the NPF being enhanced at the street site. The differences for <20 nm particles on 21 and 23 December during the NPF were also positive, supporting the NPF being enhanced at the street site. NPF in these two days didn't detail description because they were weak and cannot allow mining more evidences.

### 3.4 Analysis of NPF being enhanced at the street site

Varying NPF rates, sulfuric acid concentrations and condensation sinks during the two measurement campaigns were shown in Fig. 8 and analyzed. Although the estimated concentrations of sulfuric acid ($SO_2$ data only on the rooftop were available) were the highest on the rooftop in December when the calculated condensation sinks were comparable to those in April, the corresponding NPF rates were the smallest. It is well known that nucleation of sulfuric acid enhanced by organics dominantly determine NPF rates in the urban atmosphere (Zhang et al., 2004, 2009, 2010; Wang et al., 2010). The smallest

Atmos. Chem. Phys. Discuss., doi:10.5194/acp-2016-1143, 2017
Manuscript under review for journal Atmos. Chem. Phys.
Published: 2 January 2017




NPF rates at the rooftop site in December can be due to the lack of sufficient low-volatility organics or amines, which were possibly associated with low biogenic emissions at the low ambient temperature.

Relative to the rooftop site, the largely increased NPF rates at the street site in December were unlikely due to the increased concentrations of sulfuric acid. Our arguments were presented as below: 1) using the measurements in April as a reference, the concentrations of sulfuric acid were probably lower at the street site than at the rooftop site on basis of lower NPF rates and larger condensation sinks at the street site; the scavenging effect should also occur in December and lower the concentrations of sulfuric acid at the street site; 2) the mixing ratios of $SO_2$ at the rooftop site in December were much larger than those in April. The sulfur content in the gasoline and diesel was limited to be below 50 ppm at that time. Thus, the $SO_2$ contributed from on-road vehicles should be negligible, comparing to the background concentration of $SO_2$ in December even at the street site.

Combining possibly low emissions of biogenic precursors in December, stronger condensational sinks and larger NPF rates at the street site in December, we inferred that NPF enhanced at the street site in December was very likely due to the nucleation of $H_2SO_4$ enhanced by additional chemicals such as organics and amines from vehicle emissions. This needs further investigation because no chemical composition data in newly formed particles were available currently.

### 3.5 Limiting factors for the growth of new particles

The two particle growth patterns in NPF events were further discussed. The new particles in Class I and Class II may exert severe health problems to human beings considering its large PNC. At the meantime, the new particles in Class I could potentially have impact on climate through radiation feedback. Theoretically, the GR of new particles is largely dependent on the amount of condensable vapors conquering over the thermodynamic force plus Kelvin Effect. The amounts of condensable vapors were determined by the emission rates of vapor precursors, photochemical reactions of the precursors and scavenging rates through the gas-particle condensation and deposition.

In Class I which was observed only in April, sulfuric acid condensation was estimated to account for only 2.3%-18% of the new particle growth, which was consistent with previous studies in Finland and Mexico (Smith, et al., 2008). All NPF

Atmos. Chem. Phys. Discuss., doi:10.5194/acp-2016-1143, 2017
Manuscript under review for journal Atmos. Chem. Phys.
Published: 2 January 2017




events in December were subject to Class II when the estimated concentrations of sulfuric acid were larger than that in April. It is reasonable to say, therefore, sulfuric acid was not the crucial species in determining two particle growth patterns.

As reported in the literature, the oxidation products of biogenic organic gases likely overwhelmingly determined the condensation growth of newly formed particles between 10-50 nm (Riipinen et al., 2011; Pierce et al., 2012; Ehn et al., 2014; Liu et al., 2014). No apparent growth of newly formed particles at ~11 nm in Class II in December was possibly related to low biogenic emissions of organic gases. The hypothesis was not applicable for Class II in April. NPF events in April occurred in sunny, windy and warm days, regardless of Class I and Class II. Moreover, there were no significant difference for condensation sinks between in Class I and Class II, suggesting that the scavenging effect may not be the key factor in determining the presence or absence of the apparent new particle growth. To further understand the mechanism modulating the differences between Class I and Class II, photochemical reactions are discussed as follows. As shown in Fig. 2, the mixing ratio of ($NO_2$+$O_3$) in Class I was generally larger than that in Class II, indicating that Class II in April may be related to weaker photochemical reactions, albeit uncertainty exists (i.e., the mixing ratio of ($NO_2$+$O_3$) was 40-50 ppb on 12 April concomitant with particle growth, comparable to that in Class II).

When four NPF events in Class I were examined, the observed growth rates of > 10 nm new particles were very low (0-0.6 nm $h^{-1}$) in the initial 20-70 minutes and then rapidly increased to 2.2-9.3 nm $h^{-1}$ in the next 2-7 hours (Fig. S2). The smooth variations of $NO_2$+$O_3$ cannot explain the sudden and rapid growth of new particles after the initial 20-70 minutes. Alternatively, the sudden shift of the gas-particle system equilibrium seemed to be the reason. When the product of gases started to be larger than the thermodynamic equilibrium constant plus the Kelvin Effect term, the reaction should proceed to the solid state, leading to the sudden growth of new particles. This also implies that semi-volatile species may play a role in the particle growth.

As mentioned earlier, there was no evident difference for the NPF rates between Class I and Class II in April. It can be inferred that the organics driving the apparent growth of > 10 nm new particles were probably different from the organics involved in nucleation (Kulmala and Kerminen, 2008; Zhang et al., 2010). That also applies to the case without obvious growth of new particles with the increased NPF rates at the street site in December.

Atmos. Chem. Phys. Discuss., doi:10.5194/acp-2016-1143, 2017
Manuscript under review for journal Atmos. Chem. Phys.
Published: 2 January 2017




Again, it is difficult to detect the organic and inorganic species in 10-50 nm particles (Smith, et al., 2008; Yue et al., 2010; Bzdek et al., 2012). The same can be said to confirm the actual organics driving the growth of >10 nm new particles.

### 3.6 Relationship between NPF rate and new particle yield

Sulfuric acid vapor has been identified as a key component for nucleation in urban atmospheres (Weber et al., 1996; Kulmala, 2003; Berndt et al., 2005; Fiedler et al., 2005). Supposed that sulfuric acid vapor are completely nucleated, followed by the nucleated particles growing to the detectable size, the yields of newly formed particles are determined mainly by the supply of sulfuric acid vapor and are less affected by the formation rate. However, it will take a long time to completely convert sulfuric acid vapor to new particles in a slow formation rate. In the atmosphere, sulfuric acid, newly formed clusters and particles can be largely scavenged by preexisting particles. The increased formation rate favors coagulation growth of <8 nm new particles, shortening the time of new particles growing to be over 8 nm (detectable in this study) and therefore increase the conversion efficiency of sulfuric acid vapor to >8 nm particles. How the increased formation rate affect the production of > 8 nm particles were examined as below:

1) The NPF rate was increased by ~3 times at the street site relative to the rooftop site on 22 December 2011. This resulted in additional increase of nucleation mode PNC by $4.9\times10^3$ particle $cm^{-3}$, equal to 50% of the NMIoNP at the rooftop site; 2) The NPF rates at the street site were increased by ~4-5 times relative to the rooftop site on 21 and 23 December 2011. This led to additional increase of new particles by $1.1\times10^3$ particle $cm^{-3}$ (equal to 24% of the NMIoNP at the rooftop site) and $2.1\times10^3$ particle $cm^{-3}$ (equal to 46% of the NMIoNP at the rooftop site), respectively. The largely increased NPF rates apparently yielded a small influence on the NMIoNP.

To further exploring the relationship between NPF rate and new particle yield, we summarized 139 cases of NPF events (only four short-term events in this study being included, all the others were subject to long-term events) from our published and unpublished database measured in Beijing, Qingdao and marginal seas of China, etc. (Fig. 9, Liu et al., 2014; Zhu et al., 2014; Man et al., 2015; Guo et al., 2016). The absolute values of the observed NPF rates implied that the NPF events had been enhanced in different extents, comparing to theoretical nucleation processes of sulfuric acid-$H_2O$ and sulfuric acid-$NH_3$-$H_2O$ (Zhang et al., 2010, Kulmala et al., 2013). The NPF rates and the NMIoNP had a good correlation only under NPF

Atmos. Chem. Phys. Discuss., doi:10.5194/acp-2016-1143, 2017
Manuscript under review for journal Atmos. Chem. Phys.
Published: 2 January 2017




rates ≤8 particle $cm^{-3}$ $s^{-1}$, with r=0.76 and p<0.01. For the NPF rates >8 particle $cm^{-3}$ $s^{-1}$, the two variables had no correlation. Both of the two variables were determined by the concentration of sulfuric acid vapor and additional organics vapor involved in nucleation, but the actual extent could highly vary in various atmospheric conditions. For the NPF rates >8 particle $cm^{-3}$ $s^{-1}$, a possible interpretation is: the concentration of additional organics vapor appeared to overwhelmingly determine the NPF rates, but the NMIoNP appeared to be determined mainly by the concentration of sulfuric acid vapor instead of additional organics. For NPF rates ≤8 particle $cm^{-3}$ $s^{-1}$, the two variables were possibly determined by both the concentration of sulfuric acid vapor and additional organics. When the NPF rates was increased from 1 to 8 particle $cm^{-3}$ $s^{-1}$, the nucleation mode PNC was increased from $0.4\times10^4$ to $3.3\times10^4$ particle $cm^{-3}$ according to the regression equation. The statistical response of the NMIoNP to the increased NPF rate was stronger than the results observed at the street site in December. This allows speculating that the NMIoNP in most of atmospheric observations was possibly determined by the concentration of sulfuric acid vapor slightly more than additional organics. This of course needs both vapors' data and chemical composition data in nucleation mode particles to confirm in future, which is beyond our current capacity.

## 4. Conclusions

The simultaneous aerosol measurements at a street site and a rooftop site were conducted using two FMPS in 1-second time resolution during two seasons. In the springtime, NPF at the street site was found to be reduced on basis of the lower NPF rate and new particle yields relative to the rooftop site. We inferred that the reduced NPF at the street site was likely attributed to the scavenging effect where pollutants emitted from on-road vehicles were accumulated. In contrast, NPF was confirmed to be enhanced at the street site relative to the rooftop site in wintertime, characterized by 3-5 times higher in NPF rate and 24-50% increase of new particle yields. The largely increased NPF rates were argued due to the nucleation of $H_2SO_4$ enhanced by additional chemicals such as organics and amines from vehicle emissions. The in-depth analysis results suggested that the new particle yields were possibly determined slightly more by the concentration of sulfuric acid vapor than additional organics.

Two growth patterns of new particles were observed and occurred seasonally, i.e., Class I showed a clear "banana shape" growth of new particles and occurred only in spring (4 days out of 7 NPF days), while Class II showed no apparent growth

Atmos. Chem. Phys. Discuss., doi:10.5194/acp-2016-1143, 2017
Manuscript under review for journal Atmos. Chem. Phys.
Published: 2 January 2017




of new particles at ~11 nm and occurred in spring (3 days out of 7 NPF days) and in winter. Sulfuric acid can explain only 2.3%-18% of the new particle growth in Class I, and therefore are unlikely the crucial species determining two particle growth patterns. Through a comprehensive analysis, we proposed that some semi-volatile species oxidized from biogenic organics in presence of strong photochemical reactions likely played an important role in the growth of new particles > 10 nm.

**Acknowledgments**

We would like to thank the support from grant National Program on Key Basic Research Project (973 Program, 2014CB953700) and National Natural Science Foundation of China (NFSC, 41576118). We thank the instrument from Prof. Tong Zhu and valuable comments from Prof. Ming Fang.

Atmos. Chem. Phys. Discuss., doi:10.5194/acp-2016-1143, 2017
Manuscript under review for journal Atmos. Chem. Phys.
Published: 2 January 2017




**References:**

Arnold, F., Pirjola, L., Rönkkö, T., Reichl, U., Schlager, H., Lähde, T., Heikkila, J., and Keskinen, J.: First online measurements of sulfuric acid gas in modern heavy-duty diesel engine exhaust: Implications for nanoparticle formation, Environ. Sci. Technol., 46, 11227-11234, doi: 10.1021/es302432s, 2012.

Berndt, T., Böge, O., Stratmann, F., Heintzenberg, J., and Kulmala, M.: Rapid formation of sulfuric acid particles at near-atmospheric conditions, Science, 307, 698-700, doi:10.1126/science.1104054, 2005.

Bishop, G. A., Peddle, A. M., Stedman, D. H., and Zhan, T.: On-road emission measurements of reactive nitrogen compounds from three California cities, Environ. Sci. Technol., 44, 3616-3620, doi: 10.1021/es903722p, 2010.

Buccolieri, R., Gromke, C., Di Sabatino, S., and Ruck, B.: Aerodynamic effects of trees on pollutant concentration in street canyons, Sci. Total Environ., 407, 5247-5256, doi:10.1016/j.scitotenv.2009.06.016, 2009,

Burgard, D. A., Bishop, G. A., and Stedman, D. H.: Remote sensing of ammonia and sulfur dioxide from on-road light duty vehicles, Environ. Sci. Technol., 40, 7018-7022, doi: 10.1021/es061161r, 2006.

Bzdek, B. R., Zordan, C. A., Pennington, M. R., Luther III, G. W., and Johnston, M. V.: Quantitative assessment of the sulfuric acid contribution to new particle growth. Environ. Sci. Technol., 46, 4365-4373, doi:10.1021/es204556c, 2012.

Dal Maso, M., Kulmala, M., Riipinen, I., Wagner, R., Hussein, T., Aalto, P. P., and Lehtinen, K. E. J.: Formation and Growth of Fresh Atmospheric Aerosols: Eight Years of Aerosol Size Distribution Data from SMEAR II, Hyytiala, Finland, Boreal Environ. Res., 10, 323-336, 2005.

Ehn, M., Thornton, J. A., Kleist, E., Sipilä, M., Junninen, H., Pullinen, I., Springer, M., Rubach, F., Tillmann, R., Lee, B., Lopez-Hilfiker, F., Andres, S., Acir, I-H., Rissanen, M., Jokinen, T., Schobesberger, S., Kangasluoma, J., Kontkanen, J., Nieminen, T., Kurtén, T., Nielsen, L. B., Jørgensen, S., Kjaergaard, H. G., Canagaratna, M., Dal Maso, M., Berndt, T., Petäjä, T., Wahner, A., Kerminen, V-M., Kulmala, M., Worsnop, D. R., Wildt, J., and Mentel, T. F.: A large source of low-volatility secondary organic aerosol, Nature, 506, 476-479, doi:10.1038/nature13032, 2014.

Fiedler, V., Dal Maso, M., Boy, M., Aufmhoff, H., Hoffmann, J., Schuck, T., Birmili, W., Hanke, M., Uecker, J., Arnold, F., Kulmala, M.: The contribution of sulphuric acid to atmospheric particle formation and growth: a comparison between boundary layers in Northern and Central Europe, Atmos. Chem. Phys., 5, 1773-1785, doi:10.5194/acp-5-1773-2005,



2005.

Guo, T., Li, K., Zhu, Y., Gao, H., and Yao, X.: Concentration and size distribution of particulate oxalate in marine and coastal atmospheres–Implication for the increased importance of oxalate in nanometer atmospheric particles, Atmos. Environ., 142, 19-31, doi:10.1016/j.atmosenv.2016.07.026, 2016.

Ge, X., Wexler, A. S., and Clegg, S. L.: Atmospheric amines–Part I. A review, Atmos. Environ., 45, 524-546, doi.org/10.1016/j.atmosenv.2010.10.012, 2011.

Hu, B., Wang, Y., and Liu, G.: Relationship between Net Radiation and Broadband Solar Radiation in the Tibetan Plateau, Adv. Atmos. Sci., 29, 135-143, doi:10.1007/s00376-011-0221-6, 2012.

Hu, B., Wang, Y., and Liu, G.: Properties of ultraviolet radiation and the relationship between ultraviolet radiation and aerosol optical depth in China, Atmos. Res., 98, 297-308, doi:10.1016/j.atmosres.2010.07.009, 2010.

Kittelson, D. B.: Engines and nanoparticles: a review, J. Aerosol Sci., 29, 575-588, doi:10.1016/S0021-8502(97)10037-4, 1998.

Kittelson, D. B., Watts, W. F., Johnson, J. P., Thorne, C., Higham, C., Payne, M., Goodier, S., Warrens, C., Preston, H., Zink, U., Pickles, D., Goersmann, C., Twigg, M. V., Walker, A. P., Boddy, R., and Boddy, R.: Effect of fuel and lube oil sulfur on the performance of a diesel exhaust gas continuously regenerating trap, Environ. Sci. Technol., 42, 9276-9282, doi: 10.1021/es703270j, 2008.

Kulmala, M.: How particles nucleate and grow, Science, 302, 1000-1001, doi:10.1126/science.1090848, 2003.

Kulmala, M., Dal Maso, M., Mäkelä, J. M., Pirjola, L., Väkevä, M., Aalto, P., Miikkulainen, P., Hämeri, K., and O'Dowd, C. D.: On the formation, growth and composition of nucleation mode particles, Tellus B., 53, 479-490, doi: 10.1034/j.1600-0889.2001.530411.x, 2001.

Kulmala, M. and Kerminen, V. M.: On the formation and growth of atmospheric nanoparticles, Atmos. Res., 90, 132-150, doi:10.1016/j.atmosres.2008.01.005, 2008.

Kulmala, M., Kontkanen, J., Junninen, H., Lehtipalo, K., Manninen, H. E., Nieminen, T., Petäjä, T.; Sipilä, M., Schobesberger, S., Rantala, P., Franchin. A., Jokinen, T., Järvinen, E., Äijälä, M., Kangasluoma, J., Hakala, J., Aalto, P. P., Paasonen, P., Mikkilä, J., Vanhanen, J., Aalto, J., Hakola, H., Makkonen, U., Ruuskanen, T., Mauldin III, R. L.,



Duplissy, J., Vehkamäki, H., Bäck, J., Kortelainen, A., Riipinen, I., Kurtén, T., Johnston, M. V., Smith, J. N., Ehn, M., Mentel, T. F., Lehtinen, K. E., Laaksonen, A., Kerminen, V. M., Worsnop, D. R.: Direct Observations of Atmospheric Aerosol Nucleation, Science, 339, 943-946. doi: 10.1126/science.1227385, 2013.

Kulmala, M., Petäjä, T., Mönkkönen, P., Koponen, I. K., Dal Maso, M., Aalto, P. P., Lehtinen, K. E. J., and Kerminen, V. M.: On the growth of nucleation mode particles: source rates of condensable vapor in polluted and clean environments, Atmos. Chem. Phys., 5, 409-416. doi:10.5194/acp-5-409-2005, 2005.

Kulmala, M., Petäjä, T., Nieminen, T., Sipilä, M., Manninen, H. E., Lehtipalo, K., Maso, M. D., Aalto, P. P., Junninen, H., Paasonen, P., Riipinen, I., Lehtinen, K. E. J., Laaksonen, A., Kerminen, V-M., Measurement of the nucleation of atmospheric aerosol particles, Nature Protocols., 7, 1651-1667, doi:10.1038/nprot.2012.091, 2012.

Kulmala, M., Vehkamäki, H., Petäjä, T., Dal Maso, M., Lauri, A., Kerminen, V. M., Birmili, W., and McMurry, P. H.: Formation and growth rates of ultrafine atmospheric particles: a review of observations, J. Aerosol Sci., 35, 143-176, doi:10.1016/j.jaerosci.2003.10.003, 2004.

Lee, B. P., Li, Y. J., Flagan, R. C., Lo, C., and Chan, C. K.: Sizing characterization of the fast mobility particle sizer (FMPS) against SMPS and HR-ToF-AMS. Aerosol Sci. Technol., 47, 1030-1037, doi:10.1080/02786826.2013.810809, 2013

Liu, X. H., Zhu, Y. J., Zheng, M., Gao, H. W., and Yao, X. H.: Production and growth of new particles during two cruise campaigns in the marginal seas of China, Atmos. Chem. Phys., 14, 7941-7951, doi:10.5194/acp-14-7941-2014, 2014.

Man, H., Zhu, Y., Ji, F., Yao, X., Lau, N. T., Li, Y., Lee, B. P., and Chan, C. K.: Comparison of Daytime and Nighttime New Particle Growth at the HKUST Supersite in Hong Kong. Environ. Sci. Technol., 49, 7170-7178, doi:10.1021/acs.est.5b0214, 2015

Merikanto, J., Spracklen, D. V., Mann, G. W., Pickering, S. J., and Carslaw, K. S.: Impact of nucleation on global CCN, Atmos. Chem. Phys. 9(21), 8601-8616, doi:10.5194/acp-9-8601-2009, 2009.

Oberdörster, G., Sharp, Z., Atudorei, V., Elder, A., Gelein, R., Kreyling, W., and Cox, C.: Translocation of Inhaled Ultrafine Particles to the Brain, Inhalation Toxicol., 16, 437-445, doi.org/10.1080/08958370490439597, 2004.

Petäjä, T., Mauldin III, R. L., Kosciuch, E., McGrath, J., Nieminen, T., Paasonen, P., Boy, M., Adamov, A., Kotiaho, T., and Kulmala, M.: Sulfuric acid and OH concentrations in a boreal forest site., Atmos. Chem. Phys., 9, 7435-7448,



doi:10.5194/acp-9-7435-2009, 2009.

Pierson, W. R. and Brachaczek, W. W.: Emissions of ammonia and amines from vehicles on the road, Environ. Sci. Technol., 17, 757-760, doi: 10.1021/es00118a013, 1983.

Pierce, J. R., Leaitch, W. R., Liggio, J., Westervelt, D. M., Wainwright, C. D., Abbatt, J. P. D., Ahlm, L., Al-Basheer, W., Cziczo, D. J., Hayden, K. L., Lee, A. K. Y., Li, S.-M., Russell, L. M., Sjostedt, S. J., Strawbridge, K. B., Travis, M., Vlasenko, A., Wentzell, J. J. B., Wiebe, H. A., Wong, J. P. S., and Macdonald, A. M. Nucleation and condensational growth to CCN sizes during a sustained pristine biogenic SOA event in a forested mountain valley, Atmos. Chem. Phys., 12, 3147-3163, doi:10.5194/acp-12-3147-2012, 2012.

Riccobono, F., Schobesberger, S., Scott, C. E., Dommen, J., Ortega, I. K., Rondo, L., Almeida, J., Amorim, A., Bianchi, F., Breitenlechner, M., David, A., Downard, A., Dunne, E. M., Duplissy, J., Ehrhart, S., Flagan, R. C., Franchin, A., Hansel, A., Junninen, H., Kajos, M., Keskinen, H., Kupc, A., Kürten, A., Kvashin, A. N., Laaksonen, A., Lehtipalo, K., Makhmutov, V., Mathot, S., Nieminen, T., Onnela, A., Petäjä, T., Praplan, A. P., Santos, F. D., Schallhart, S., Seinfeld, J. H., Sipilä, M., Spracklen, D. V., Stozhkov, Y., Stratmann, F., Tomé, A., Tsagkogeorgas, G., Vaattovaara, P., Viisanen, Y., Vrtala, A., Wagner, P, E., Weingartner, E., Wex, H., Wimmer, D., Carslaw, K, S., Curtius, J., Donahue, N. M., Kirkby, J., Kulmala, M., Worsnop, D. R., and Baltensperger, U.: Oxidation products of biogenic emissions contribute to nucleation of atmospheric particles, Science, 344, 717-721, doi: 10.1126/science.1243527, 2014.

Riipinen, I., Pierce, J. R., Yli-Juuti, T., Nieminen, T., Häkkinen, S., Ehn, M., Junninen, H., Lehtipalo, K., Petäjä, T., Slowik, J., Chang, R., Shantz, N. C., Abbatt, J., Leaitch, W. R., Kerminen, V. M., Worsnop, D. R., Pandis, S. N., Donahue, N. M., and Kulmala, M.: Organic condensation: a vital link connecting aerosol formation to cloud condensation nuclei (CCN) concentrations, Atmos. Chem. Phys., 11, 3865-3878, doi:10.5194/acp-11-3865-2011, 2011.

Rönkkö, T., Lähde, T., Heikkilä, J., Pirjola, L., Bauschke, U., Arnold, F., Schlager, H., Rothe, D., Yli-Ojanpera, J., and Keskinen, J.: Effects of gaseous sulphuric acid on diesel exhaust nanoparticle formation and characteristics, Environ. Sci. Technol., 47, 11882-11889. doi:10.1021/es402354y, 2013.

Schlesinger, R.B., Kunzli, N., Hidy, G.M., Gotschi, T., and Jerrett, M.: The Health Relevance of Ambient Particulate Matter Characteristics: Coherence of Toxicological and Epidemiological Inferences, Inhalation Toxicol., 18, 95-125, doi:

10.1080/08958370500306016, 2006.

Schobesberger, S., Junninen, H., Bianchi, F., Lönn, G., Ehn, M., Lehtipalo, K., Dommen, J., Ehrhart, S., Ortega, I. K., Franchin, A., Nieminen, T., Riccobono, F., Hutterli, M., Duplissy, J., Almeida, J., Amorim, A., Breitenlechner, M., Downard, A. J., Dunne, E. M., Flagan, R. C., Kajos, M., Keskinen, H., Kirkby, J., Kupc, A., Kurten, A., Kurten, T., Laaksonen, A., Mathot, S., Onnela, A., Praplan, A. P., Rondo, L., Santos, F. D., Schallhart, S., Schnitzhofer, R., Sipila, M., Tome, A., Tsagkogeorgas, G., Vehkamaki, H., Wimmer, D., Baltensperger, U., Carslaw, K. S., Curtius, J., Hansel, A., Petaja, T., Kulmala, M., Donahue, N. M., and Worsnop, D. R.: Molecular understanding of atmospheric particle formation from sulfuric acid and large oxidized organic molecules, Proc. Natl. Acad. Sci., 110, 17223-17228, doi: 10.1073/pnas.1306973110, 2013.

Shi, J. P., Mark, D., and Harrison, R. M., Characterization of particles from a current technology heavy-duty diesel engine, Environ. Sci. Technol., 34, 748-755, doi: 10.1021/es990530z, 2000.

Shi, Z. B., He, K. B., Yu, X. C., Yao, Z. L., Yang, F. M., Ma, Y. L., Ma, R., Jia, Y. T., and Zhang, J.: Diurnal variation of number concentration and size distribution of ultrafine particles in the urban atmosphere of Beijing in winter, J. Environ. Sci., 19, 933-938. doi:10.1016/S1001-0742(07)60154-5, 2007.

Smith, J. N., Dunn, M. J., VanReken, T. M., Iida, K., Stolzenburg, M. R., McMurry, P. H., and Huey, L. G.: Chemical composition of atmospheric nanoparticles formed from nucleation in Tecamac, Mexico: Evidence for an important role for organic species in nanoparticle growth. Geophys. Res. Lett., 35, doi: 10.1029/2007GL032523, 2008.

Stemmler, K., Bugmann, S., Buchmann, B., Reimann, S., and Staehelin, J.: Large decrease of VOC emissions of Switzerland's car fleet during the past decade: results from a highway tunnel study. Atmos. Environ., 39, 1009-1018, doi:10.1016/j.atmosenv.2004.10.010, 2005.

Sun, Y. L., Zhang, Q., Schwab, J. J., Chen, W. N., Bae, M. S.; Hung, H. M., Lin, Y. C., Ng, N. L., Jayne, J., Massoli, P., Williams, L. R., and Demerjian, K. L.: Characterization of near-highway submicron aerosols in New York City with a high-resolution aerosol mass spectrometer, Atmos. Chem. Phys., 12, 2215-2227, doi:10.5194/acp-12-2215-2012, 2012.

Tröstl, J., Chuang, W. K., Gordon, H., Heinritzi, M., Yan, C., Molteni, U., Ahlm, L., Frege, C., Bianchi, F., Wagner, R., Simon, M., Lehtipalo, K., Williamson, C., Craven, J. S., Duplissy, J., Adamov, A., Almeida, J., Bernhammer, J. A. K.,

Breitenlechner, M., Brilke, S., Ehrhart, S., Dias, A., Flagan, R. C., Franchin, A., Fuchs, C., Guida, R., Gysel, M., Hansel, A., Hoyle, C. R., Jokinen, T., Junninen, H., Kangasluoma, J., Keskinen, H., Kim, J., Krapf, M., Kürten, A., Laaksonen, A., Lawler, M., Leiminger, M., Mathot, S., Möhler, O., Nieminen, T., Onnela, A., Petäjä, T., Piel, F. M., Miettinen, P., Rissanen, M. P., Rondo, L., Sarnela, N., Schobesberger, S., Sengupta, K., Sipilä, M., Smith, J. N., Steiner, G., Tomè, A., Virtanen, A., Wagner, A. C., Weingartner, E., Wimmer, D., Winkler, P. M., Ye, P. L., Carslaw, K. S., Curtius, J., Dommen, J., Kirkby, J., Kulmala, M., Riipinen, I., Worsnop, D. R., Donahue, N. M., and Baltensperger, U.: The role of low-volatility organic compounds in initial particle growth in the atmosphere, Nature, 533, 527-531, doi:10.1038/nature18271, 2016.

Vu, T. V., Delgado-Saborit, J. M., and Harrison, R. M.: Review: Particle number size distributions from seven major sources and implications for source apportionment studies, Atmos. Environ., 122, 114-132, doi:10.1016/j.atmosenv.2015.09.027, 2015.

Wang, L., Khalizov, A.F., Zheng, J., Xu, W., Ma, Y., Lal, V., and Zhang, R.: Atmospheric nanoparticles formed from heterogeneous reactions of organics, Nature Geosci., 3, 238-242, doi:10.1038/ngeo778, 2010.

Wang, Z., Wu, Z., Yue, D., Shang, D., Guo, S., Sun, J., Ding, A., Wang, L., Jiang, J., Guo, H., Gao, J., Cheung, H.C., Morawska, L., Keywood, M., and Hu, M.: New particle formation in China: Current knowledge and further directions, Sci. Total Environ., 577, 258-266, doi: 10.1016/j.scitotenv.2016.10.177, 2017.

Weber, R. J., Marti, J. J., McMurry, P. H., Eisele, F. L., Tanner, D. J., and Jefferson, A.: Measured atmospheric new particle formation rates: Implications for nucleation mechanisms. Chem. Eng. Commun., 151, 53-64, doi:10.1080/00986449608936541, 1996.

Wehner, B., Wiedensohler, A., Tuch, T. M., Wu, Z. J., Hu, M., Slanina, J., and Kiang, C. S.: Variability of the aerosol number size distribution in Beijing, China: New particle formation, dust storms, and high continental background, Geophys. Res. Lett., 31, doi:10.1029/2004GL021596, 2004.

Wehner, B., Birmili, W., Ditas, F., Wu, Z., Hu, M., Liu, X., Mao, J., Sugimoto, N., and Wiedensohler, A.: Relationships between submicrometer particulate air pollution and air mass history in Beijing, China, 2004-2006, Atmos. Chem. Phys., 8, 6155-6168, doi:10.5194/acp-8-6155-2008, 2008.

Whitby, K. T.: The physical characteristics of sulfur aerosols, Atmos. Environ., 12, 135-159, doi:10.1016/0004-6981(78)90196-8, 1978.

Wildt, J., Mentel, T. F., Kiendler-Scharr, A., Hoffmann, T., Andres, S., Ehn, M., Kleist, E., Müsgen, P., Rohrer, F., Rudich, Y., Springer, M., Tillmann, R., and Wahner, A.: Suppression of new particle formation from monoterpene oxidation by NOx, Atmos. Chem. Phys., 14, 2789-2804, doi:10.5194/acp-14-2789-2014, 2014.

Wu, Z., Hu, M., Liu, S., Wehner, B., Bauer, S., Ma ßling, A., Wiedensohler, A., PetäJä, T., Dal Maso, M., and Kulmala, M.: New particle formation in Beijing, China: Statistical analysis of a 1 - year data set, J. Geophys. Res., 112, doi: 10.1029/2006JD007406, 2007.

Yao, X., Chan, C. K., Lau, N. T., Lau, P. S., and Fang, M.: Possible sampling artifact in real time particle size distributions related to sampling rate, Aerosol Sci. Technol., 40, 1080-1089, doi: 10.1080/02786820600979121, 2006a.

Yao, X. H., Lau, N. T., Fang, M., and Chan, C. K.: On the time-averaging of ultrafine particle number size spectra in vehicular plumes, Atmos. Chem. Phys., 6, 4801-4807, doi:10.5194/acp-6-4801-2006, 2006b.

Yao, X., Lau, N. T., Fang, M., and Chan, C. K.: Real-time observation of the transformation of ultrafine atmospheric particle modes, Aerosol Sci. Technol., 39, 831-841, doi:10.1080/02786820500295248, 2005.

Yue, D. L., Hu, M., Zhang, R. Y., Wang, Z. B., Zheng, J., Wu, Z. J., Wiedensohler, A., He, L. Y., Huang, X. F., and Zhu, T.: The roles of sulfuric acid in new particle formation and growth in the mega-city of Beijing, Atmos. Chem. Phys., 10, 4953–4960, doi:10.5194/acp-10-4953-2010, 2010.

Zimmerman, N., Jeong, C. H., Wang, J. M., Ramos, M., Wallace, J. S., and Evans, G. J.: A source-independent empirical correction procedure for the fast mobility and engine exhaust particle sizers, Atmos. Environ., 100, 178-184, doi.org/10.1016/j.atmosenv.2014.10.054, 2015.

Zhang, R.: Getting to the Critical Nucleus of Aerosol Formation. Science, 328, 1366-1367, doi: 10.1126/science.1189732, 2010,

Zhang, R., Khalizov, A., Wang, L., Hu, M., and Xu, W.: Nucleation and growth of nanoparticles in the atmosphere, Chem. Rev., 112, 1957-2011, doi: 10.1021/cr2001756, 2012.

Zhang, R., Suh, I., Zhao, J., Zhang, D., Fortner, E. C., Tie, X., Molina, L. T., and Molina, M. J.: Atmospheric new particle

formation enhanced by organic acids. Science, 304, 1487-1490, doi:10.1126/science.1095139, 2004.

Zhang, R., Wang, G., Guo, S., Zamora, M. L., Ying, Q., Lin, Y., Wang, W., Hu, M., and Wang, Y.: Formation of Urban Fine Particulate Matter, Chem. Rev., 115, 3803-3855, doi:10.1021/acs.chemrev.5b00067, 2015.

Zhang, R., Wang, L., Khalizov, A. F., Zhao, J., Zheng, J., McGraw, R. L., and Molina, L.T.: Formation of nanoparticles of blue haze enhanced by anthropogenic pollution, Proc. Natl. Acad. Sci, 106, 17650-17654, doi:10.1073/pnas.0910125106, 2009.

Zhu, Y., Hinds, W.C., Kim, S., and Sioutas, C.: Concentration and size distribution of ultrafine particles near a major highway, J. Air Waste Manag. Assoc., 52, 1032-1042, doi:10.1080/10473289.2002.10470842, 2002a.

Zhu, Y., Hinds, W. C., Kim, S., Shen, S., and Sioutas, C.: Study of ultrafine particles near a major highway with heavy-duty diesel traffic, Atmos. Environ., 36, 4323-4335, doi:10.1016/S1352-2310(02)00354-0, 2002b.

Zhu, Y., Kuhn, T., Mayo, P., and Hinds, W. C.: Comparison of daytime and nighttime concentration profiles and size distributions of ultrafine particles near a major highway, Environ. Sci. Technol., 40, 2531-2536, doi:10.1021/es0516514, 2006.

Zhu, Y. J., Sabaliauskas, K., Liu, X. H., Meng, H., Gao, H. W., Jeong, C-H., Evans, G., and Yao, X. H.: Comparative analysis of new particle formation events in less and severely polluted urban atmosphere, Atmos. Environ., 98, 655-664, doi:10.1016/j.atmosenv.2014.09.043, 2014.

Atmos. Chem. Phys. Discuss., doi:10.5194/acp-2016-1143, 2017
Manuscript under review for journal Atmos. Chem. Phys.
Published: 2 January 2017


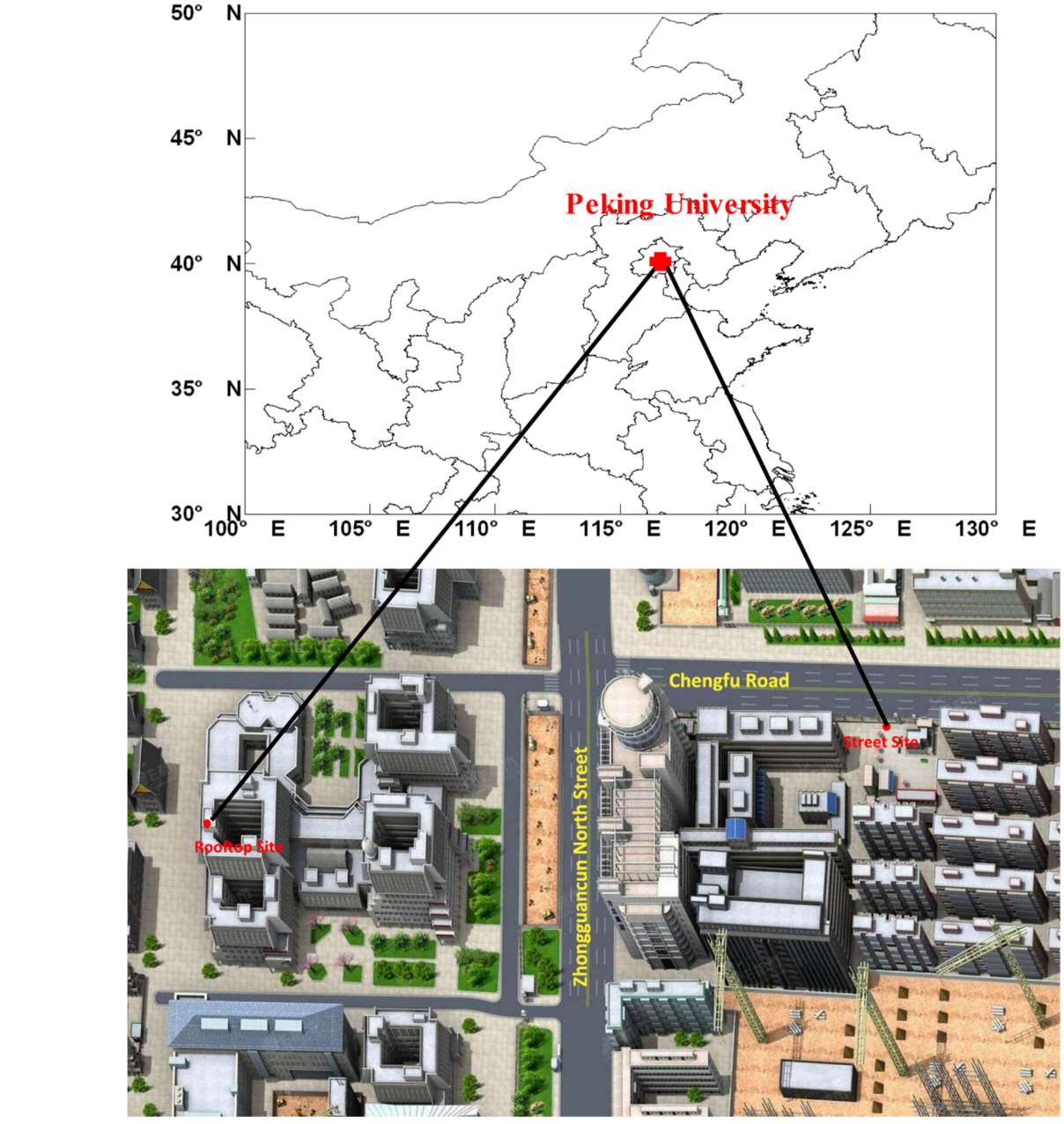


**Fig. 1** The location of sampling sites (top) and 3D view of the sites (bottom, download from http://bj.o.cn/).

Atmos. Chem. Phys. Discuss., doi:10.5194/acp-2016-1143, 2017
Manuscript under review for journal Atmos. Chem. Phys.
Published: 2 January 2017


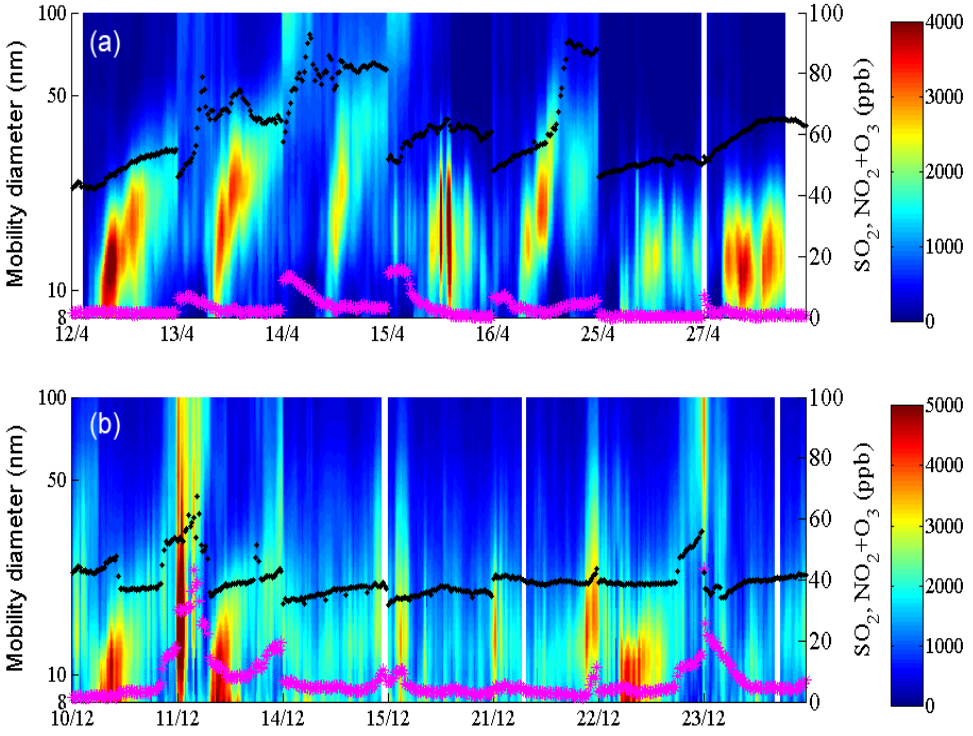


**Fig. 2** The time series from 8:00 to 18:00 of each NPF day and the variation of $NO_2$+$O_3$ and $SO_2$ (date marked at the beginning of each day. The mixing ratios of $NO_2$+$O_3$ and $SO_2$ in each event were superimposed on top of the shading in black dots and magenta stars, respectively, with corresponding values indicated on the right Y Axis).

Atmos. Chem. Phys. Discuss., doi:10.5194/acp-2016-1143, 2017
Manuscript under review for journal Atmos. Chem. Phys.
Published: 2 January 2017


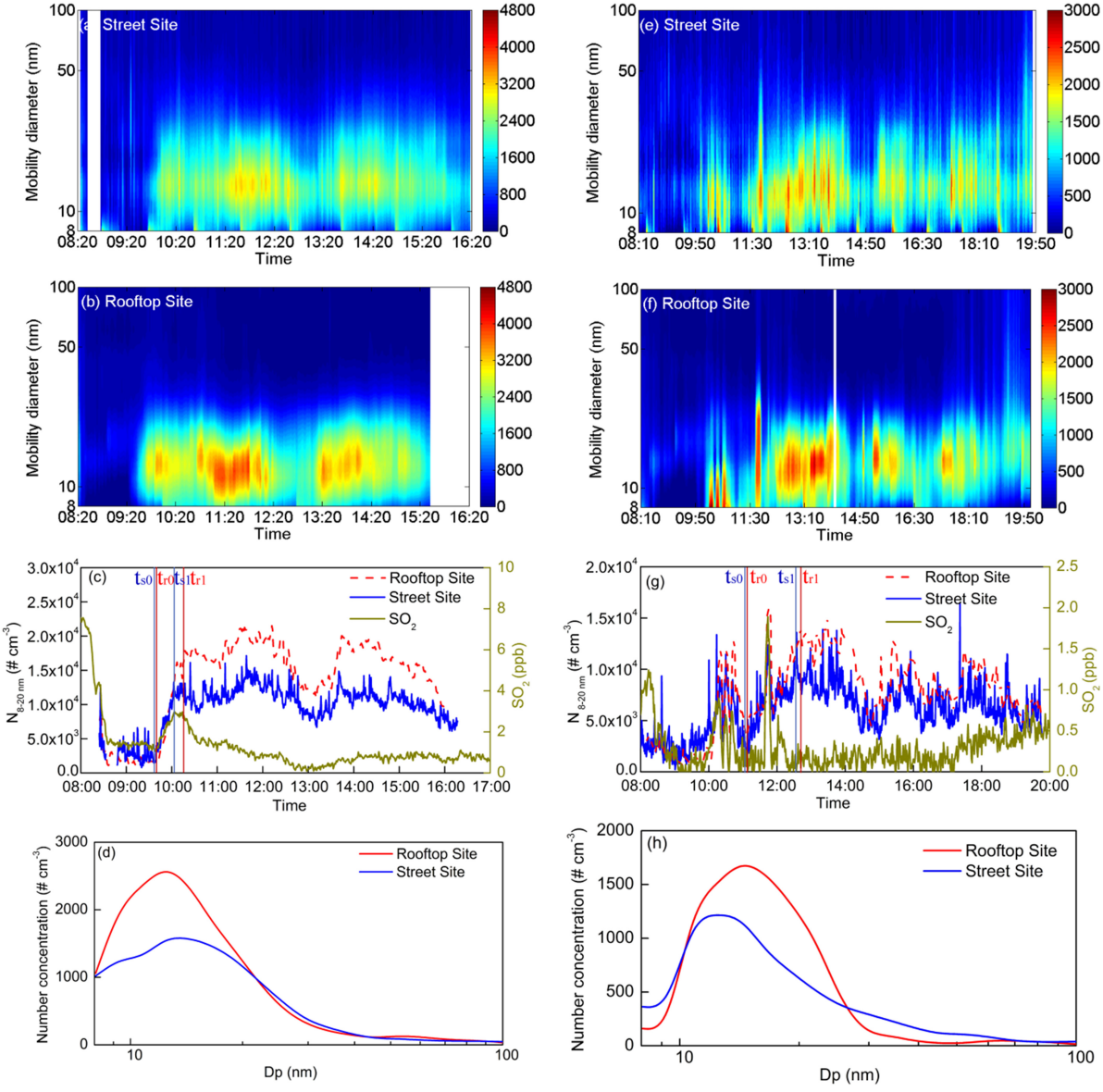


**Fig. 3** Number concentrations and size distributions of atmospheric particles at two sampling sites on 27 April 2012 (left column) and 25 April 2012 (right column) (a, b, e, f: Contour plots of particle number concentration (# $cm^{-3}$); c, g: time series of nucleation mode PNC ($N_{8\text{-}20nm}$) at two sampling sites in solid blue and dashed red, respectively (left Y Axis) and $SO_2$ mixing ratio (right Y Axis); d, h: net increase of particles size distributions inside street canyon ($t_{s1}$-$t_{s0}$) and on the rooftop ($t_{r1}$-$t_{r0}$).

Atmos. Chem. Phys. Discuss., doi:10.5194/acp-2016-1143, 2017
Manuscript under review for journal Atmos. Chem. Phys.
Published: 2 January 2017


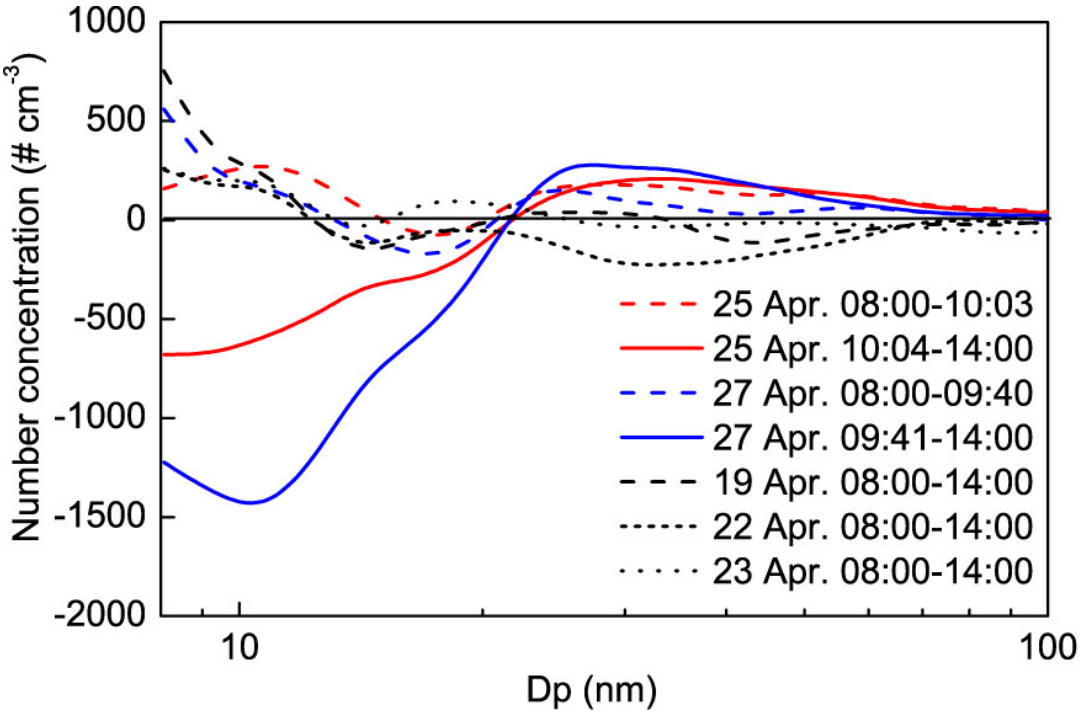


**Fig. 4** The difference of particle number concentrations between the two sites in April 2012 (The number concentrations at the street site subtracting the corresponding concentration at the rooftop site, colored and black lines representing NPF days and non-NPF days, respectively. The morning rush hours on 25 and 27 April prior to the occurrence of NPF events were listed separately).

Atmos. Chem. Phys. Discuss., doi:10.5194/acp-2016-1143, 2017
Manuscript under review for journal Atmos. Chem. Phys.
Published: 2 January 2017


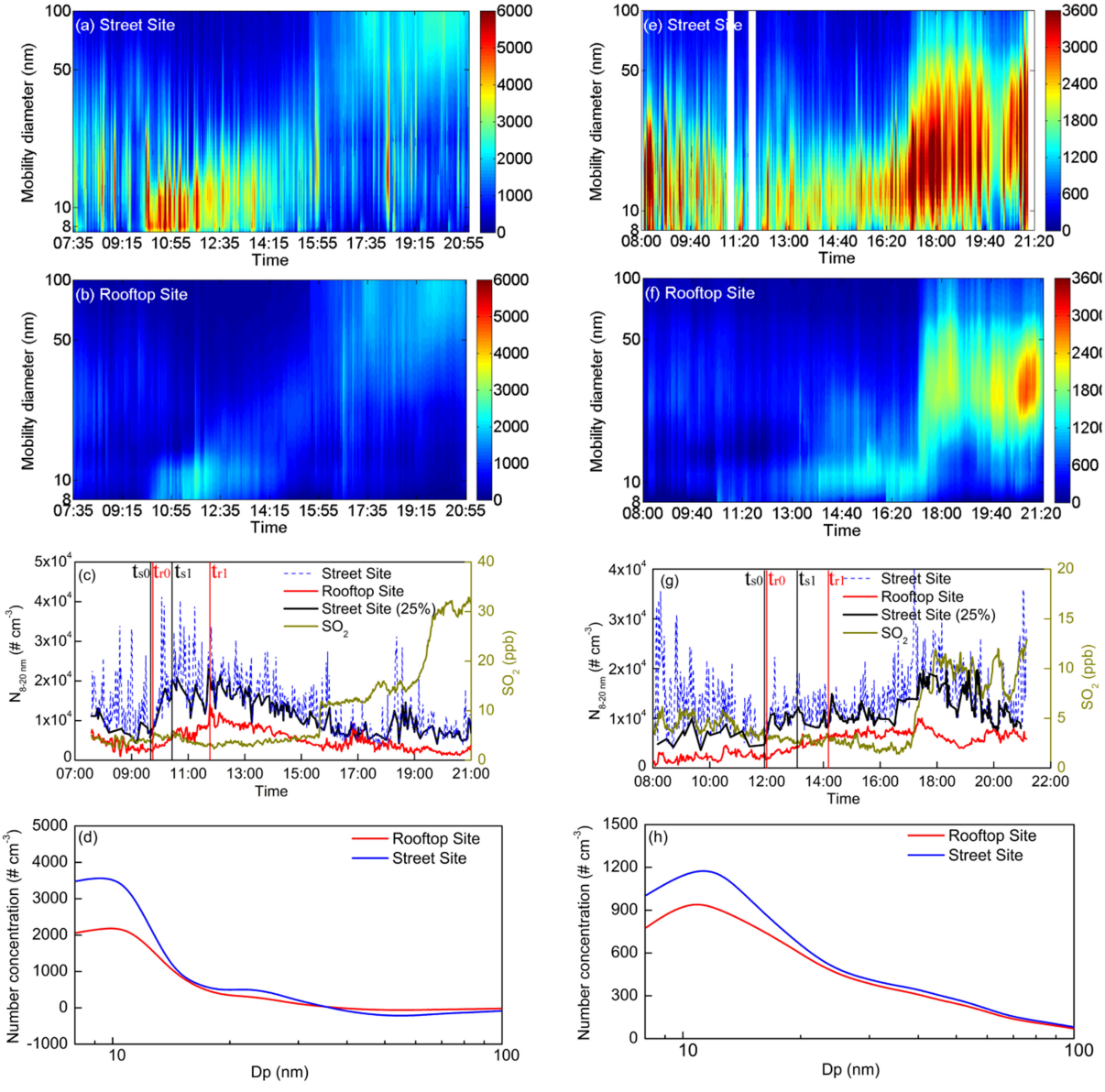


**Fig. 5** Number concentrations and size distributions of atmospheric particles at two sampling sites on 22 Decemebr 2011 (left column) and 21 Decemebr 2011 (right column) (a, b, e, f: Contour plots of particle number concentration (# $cm^{-3}$); c, g: time series of nucleation mode PNC ($N_{8\text{-}20nm}$) and $SO_2$ mixing ratios; black solid line represents those data for which the coefficient of variation in every 60 seconds was subject to the minimum 25%; d, h: net increase of particles size distributions inside street canyon ($t_{s1}$-$t_{s0}$) and on the rooftop ($t_{r1}$-$t_{r0}$)).

Atmos. Chem. Phys. Discuss., doi:10.5194/acp-2016-1143, 2017
Manuscript under review for journal Atmos. Chem. Phys.
Published: 2 January 2017


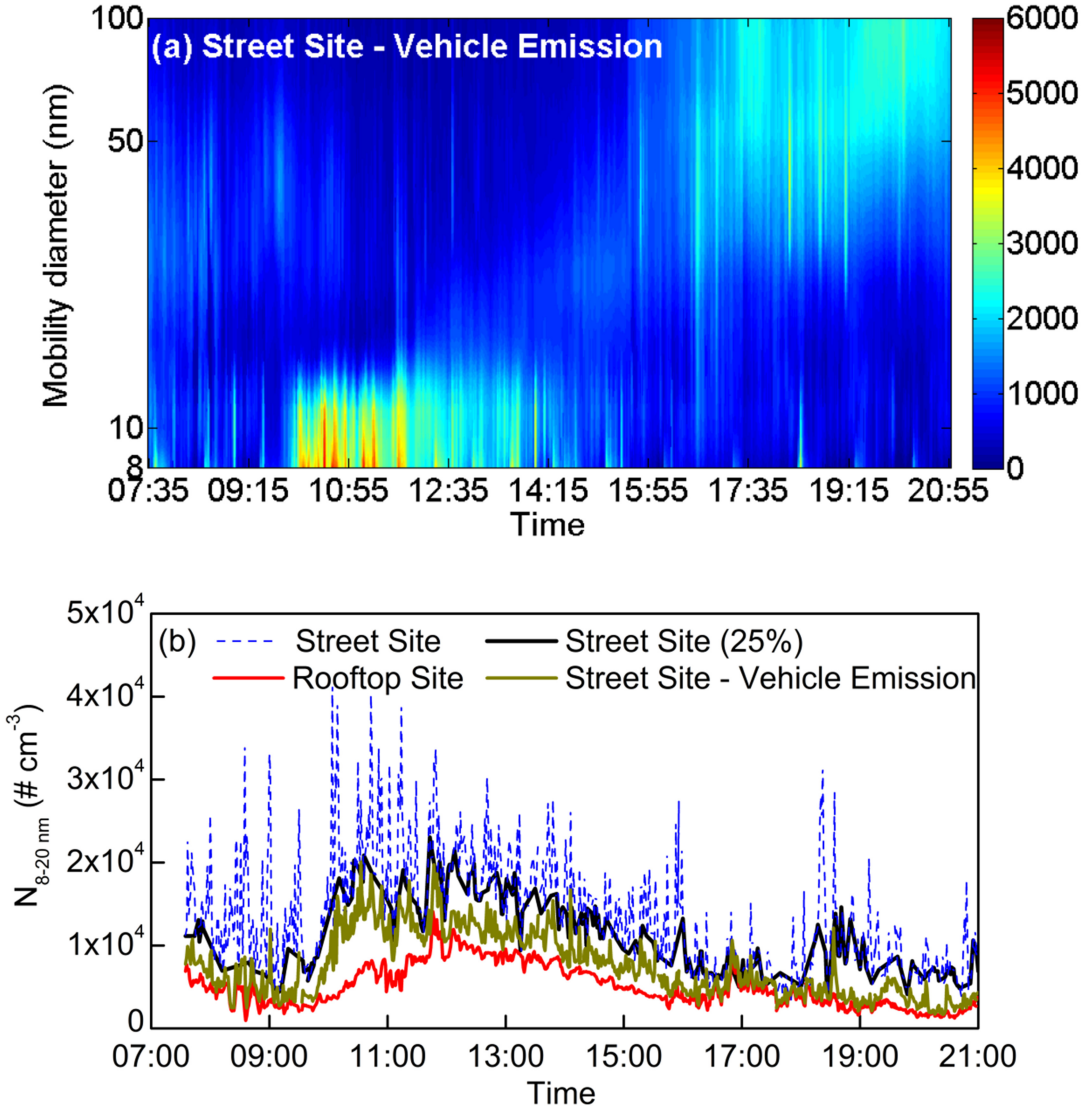


**Fig. 6** The number concentration of atmospheric particles after removing the contribution of vehicle spikes at street site on 22 December 2011 (b: yellow solid line represents the number concentration without the vehicle spikes, the remaining three lines are same as fig. 5c).

Atmos. Chem. Phys. Discuss., doi:10.5194/acp-2016-1143, 2017
Manuscript under review for journal Atmos. Chem. Phys.
Published: 2 January 2017


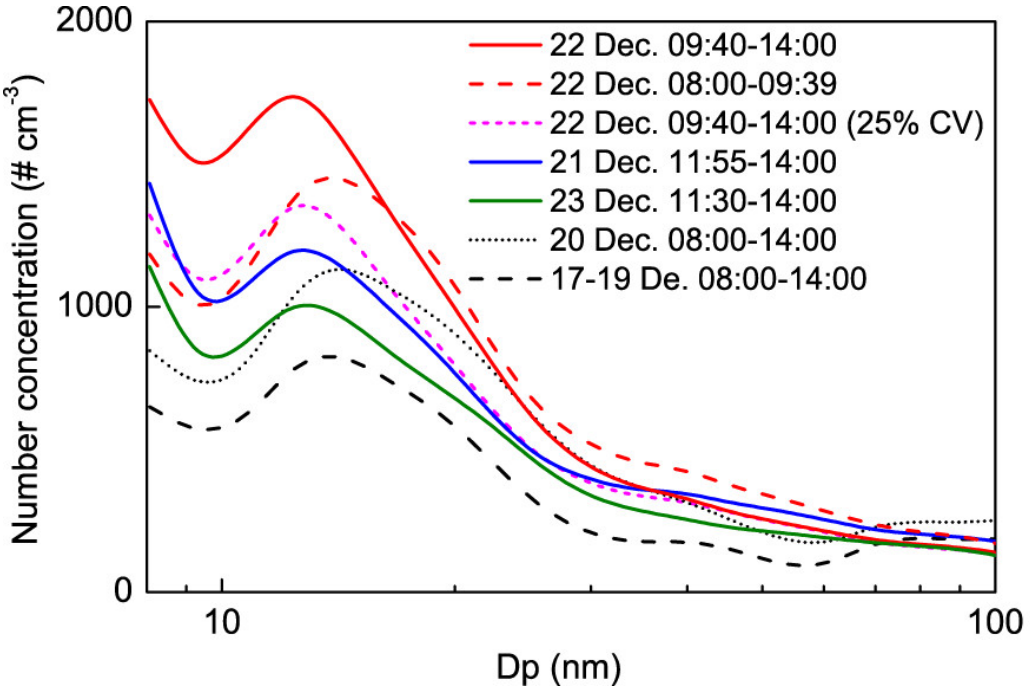


605

**Fig. 7** The difference of particle number concentrations between the two sites in December, 2011 (Color lines and black lines represent NPF days and non-NPF days. The morning rush hours on 22 December prior to the occurrence of NPF events were listed separately; magenta dash line represents those data for which the coefficient of variation in every 60 seconds was subject to the minimum 25%).

Atmos. Chem. Phys. Discuss., doi:10.5194/acp-2016-1143, 2017
Manuscript under review for journal Atmos. Chem. Phys.
Published: 2 January 2017


Atmospheric Chemistry and Physics Discussions

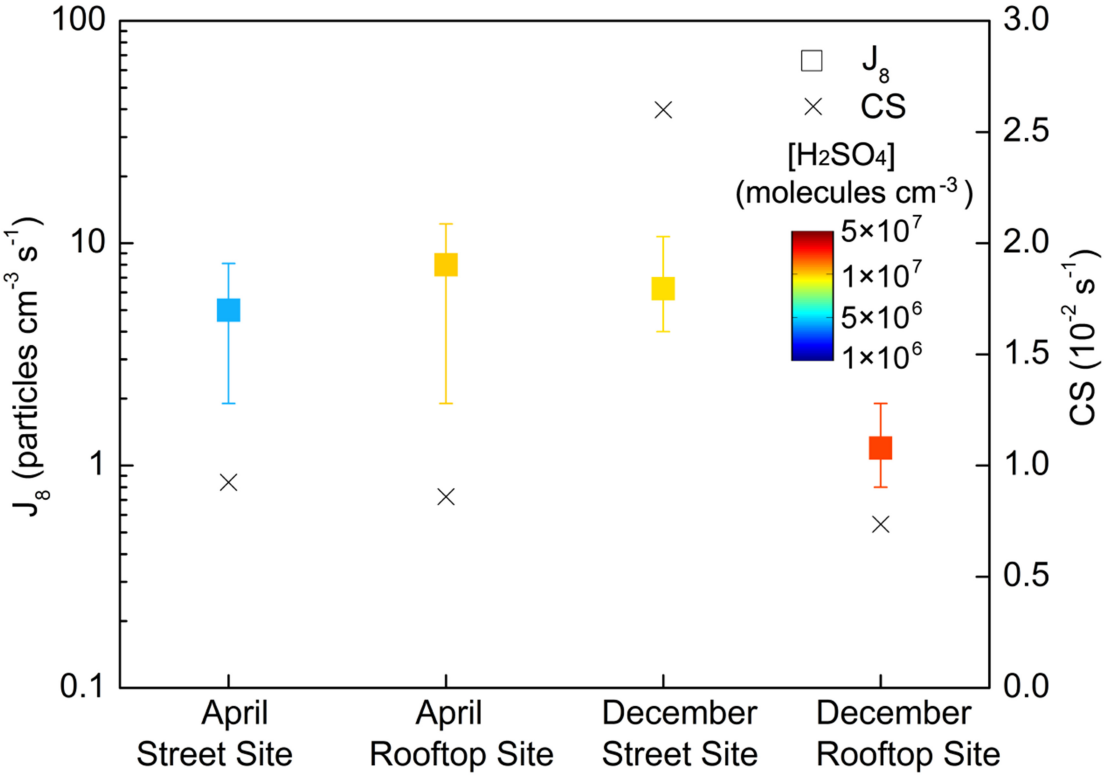


610

**Fig. 8** Mean and range of NPF rate (box symbol), condensation sinks (cross symbol) and averaged sulfuric acid concentrations (color bar) on NPF days at two sites in April and December.

Atmos. Chem. Phys. Discuss., doi:10.5194/acp-2016-1143, 2017
Manuscript under review for journal Atmos. Chem. Phys.
Published: 2 January 2017


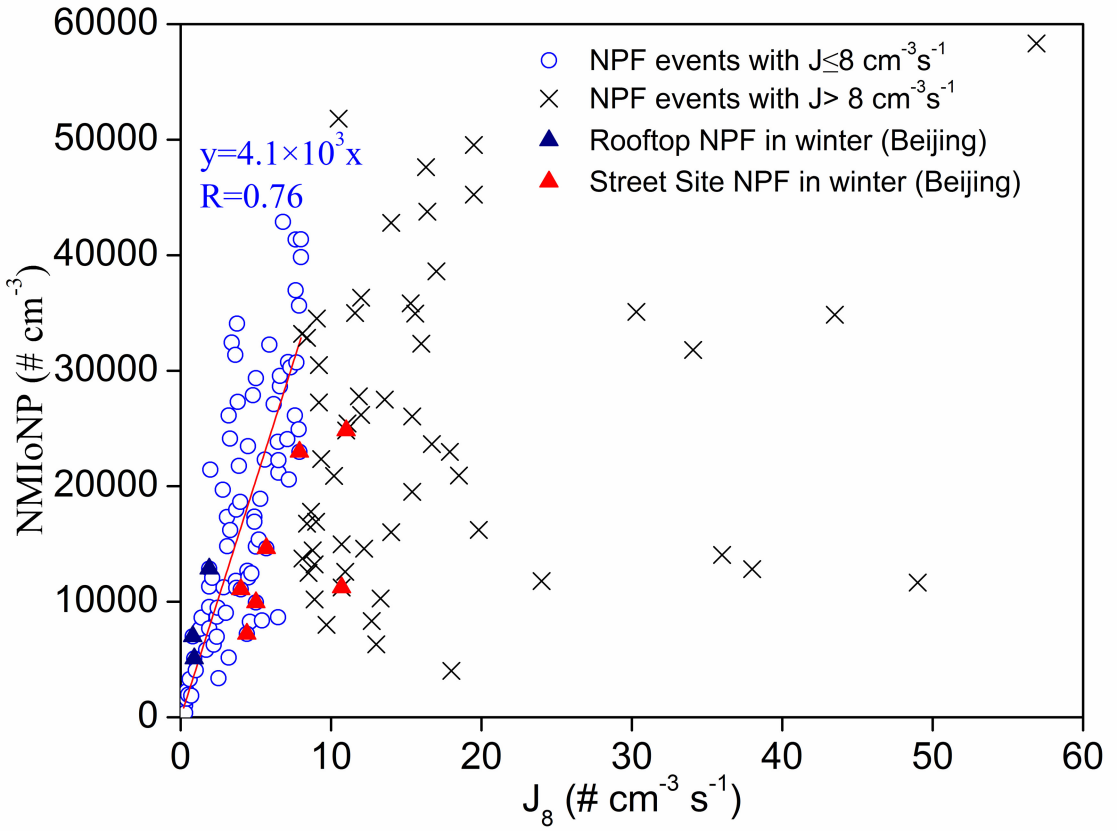


615 **Fig.9** Relationship between NPF rate ($J_8$) and net maximum increase of nucleation mode PNC (NMIoNP) in 139 cases of NPF events.